

## Phase transitions of $n\text{-C}_{32}\text{H}_{66}$ measured by means of high resolution and super-sensitive DSC

Ken-ichi Tozaki<sup>a</sup>, Hideaki Inaba<sup>a,\*</sup>, Hideko Hayashi<sup>a</sup>, Chanhji Quan<sup>a</sup>,  
Norio Nemoto<sup>b</sup>, Tsunehisa Kimura<sup>c</sup>

<sup>a</sup> Faculty of Education, Chiba University, 1-33 Yayoi-chiba, Inage-ku, Chiba 263-8522, Japan

<sup>b</sup> Department of Molecular and Material Sciences, IGSES, Kyushu University, Hakozaki, Fukuoka 812-8581, Japan

<sup>c</sup> Faculty of Technology, Tokyo Metropolitan University, Minamiosawa, Hachioji, Tokyo 192-0397, Japan

Received 10 April 2002; accepted 1 May 2002

### Abstract

A high resolution and super-sensitive differential scanning calorimetry (DSC) has been constructed by using two kinds of semi-conducting thermoelectric modules; one is used as a high-sensitive heat flow sensor and the other is for a main heater or cooler using the Peltier effect. The baseline fluctuation of the calorimeter was within  $\pm 25$  nW. Thermal analysis of  $n\text{-C}_{32}\text{H}_{66}$  was conducted using this DSC and two large peaks due to the solid-solid transition at 339.1 K from the crystalline phase to the rotator phase and the melting transition at 341.9 K were observed at the heating rate of  $0.4\text{ mK s}^{-1}$ . In addition, a small peak was detected first by DSC at 338.1 K, indicating a high sensitivity of this DSC. In the solidifying process from the melting state at the cooling rate of  $40\text{ }\mu\text{K s}^{-1}$ , several small exothermic sub-peaks were observed in addition to the main solidifying peak. © 2002 Elsevier Science B.V. All rights reserved.

**Keywords:** DSC;  $n$ -Alkane; Phase transition; High sensitivity

### 1. Introduction

Differential scanning calorimetry (DSC) [1–4] has given important information in the fields of polymer science, biological and medical science, metal science, inorganic science and their related industries by measuring a melting point, glass transition, phase transitions, enthalpy of phase transitions, heat capacity and heat generated or absorbed by chemical reaction. In the heat flux DSC [1–4], the heating rate of a metal block including the sample and the reference sample is controlled to be constant and the temperature difference

between a sample and a reference sample, when heat is generated from or absorbed in the sample, is detected and converted to heat flux using a proper calibration.

A high-sensitive and high resolution DSC capable of measuring a small heat at a slower heating rate with a small baseline fluctuation using a small sample has been increasingly demanded in various fields. In the usual DSC, the heating rate is usually chosen to be larger than  $0.1\text{ K min}^{-1}$  in order to obtain a significant signal, since the magnitude of the signal is proportional to the heating rate. It is desirable, however, to develop a high resolution and high-sensitive DSC capable of measuring at a slower heating rate, for example, less than  $0.01\text{ K min}^{-1}$  ( $0.167\text{ mK s}^{-1}$ ), with a temperature resolution of 1 mK and a baseline fluctuation less than 25 nW, since phase transitions

\* Corresponding author. Tel.: +81-43-290-2599;  
fax: +81-43-290-2519.  
E-mail address: inabah@e.chiba-u.ac.jp (H. Inaba).

between a small temperature interval can be hardly resolved at a high heating rate. The high-sensitivity of the calorimeter makes it possible to reduce the sample amount, which improves the temperature homogeneity of the sample during the measurement. It is also desirable to develop a new DSC capable of measuring in the both direction of heating and cooling near room temperature, since some sorts of materials in the cooling process often show a different behavior from the heating process. Since the cooling speed is limited by the heat loss to the surroundings and it becomes small near room temperature, a cooling device is necessary in order to obtain a precise cooling control. One of the driving forces to develop the high resolution and super-sensitive DSC is to detect a very small effect of diamagnetic substances under a strong magnetic field, which we would like to show in the next paper [5].

The *n*-alkanes have a relatively simple chemical formula,  $C_nH_{2n+2}$ , but they have structurally different phases depending on temperature and the carbon number *n* for  $C_nH_{2n+2}$  [6–19]. For *n*-alkanes with the number *n* > 20, the crystals undergo solid-solid phase transitions from a low temperature ordered phase to characteristic high temperature phases called as rotator phases. The rotator phases have three-dimensional positional order of the molecules, but lack the long-range order in the rotational degrees of freedom of the molecules about their long axes. Urabe and Takamizawa [8] showed the phase diagram of the *n*-alkanes:  $C_nH_{2n+2}$  ( $20 \leq n \leq 80$ ) using the results by DSC. Denicolo et al. [10] made a X-ray scattering study on the rotator phases for even-numbered *n*-alkanes. More recently, Sirota et al. [11] made a detailed X-ray scattering study on the rotator phases for *n*-alkanes:  $C_nH_{2n+2}$  ( $20 \leq n \leq 33$ ). They showed the phase diagram including the five rotator phases, where the lattice distortion, the molecular tilt and the Azimuthal ordering are different and they are characterized as the order parameters. They [12] also made a calorimetric study on the phase transitions for *n*-alkanes:  $C_nH_{2n+2}$  ( $20 \leq n \leq 30$ ) using an adiabatic scanning calorimeter and found rotator to rotator transitions corresponding to the rotator phases found by the X-ray scattering study. However, their measurement was limited up to  $C_{30}H_{62}$  ( $n = 30$ ) for the alkanes shown by  $C_nH_{2n+2}$ .

In the present paper, we have developed a new high resolution and super-sensitive DSC capable of

detecting a small heat at a heating and cooling rate as low as  $2.4 \text{ mK min}^{-1}$  ( $40 \mu\text{Ks}^{-1}$ ) within a baseline fluctuation of 25 nW and have found the phase transitions of  $C_{32}H_{66}$  using the calorimeter.

## 2. Experimental

### 2.1. Apparatus

The schematic drawing of the new high resolution and super-sensitive DSC is shown in Fig. 1. The measurement can be made in either direction of heating or cooling with this apparatus. The temperature difference between a test sample and a reference one, produced by the heat absorbed in or released from the sample, is measured by thermoelectric modules (Ferro. Tech. Inc., 9500/018/012), TM1 and TM2, which are made of 18 semi-conducting thermoelectric elements connected in series. The output voltage of each thermoelectric module is about  $7.8 \text{ mV K}^{-1}$ . Such a high voltage signal per a temperature change is one of the merits of this calorimeter. The temperature of the sample cell was controlled two-fold; a rough control and a precise one. The rough control was made using a Pt temperature sensor, TS3, by adjusting the power of a heater mounted on an outer cylindrical metal block. The precise control was made using a Pt temperature sensor, TS2, by adjusting the current of the thermomodule, TM3. TM3 is made of semi-conducting thermoelectric elements and can pump heat in either direction to heat or cool the copper blocks by changing the direction of the current through it. The copper blocks, B1, B2 and B3, and the thermomodule, TM2, work as heat sinks and heat resistances in this calorimeter. The combination of the heat sinks and heat resistances is considered to form the combination of condensers and resistances in an equivalent electronic circuit and reduces the temperature fluctuation produced at the base copper block, B3 and increases the stability of the calorimeter. This is another reason for the merits of this calorimeter. The stability of the baseline was measured as the difference of the electromotive force between TM1 and TM2, which was converted as heat flux through calibration. In order to check the stability of the apparatus, the variations of the temperatures at about 303 K were measured and are shown in Fig. 2. As seen in Fig. 2, the

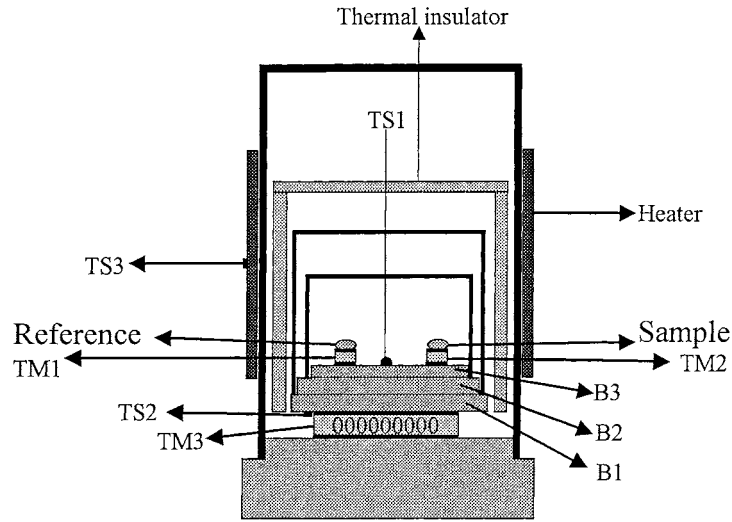


Fig. 1. Schematic drawing of the new high resolution and super-sensitive DSC.

temperature detected with TS3, was controlled to be within  $\pm 1$  mK, and that by TS2, whose fluctuation of temperature becomes small due to the dumping effect of the combination of the insulating thermal shield and

the copper disk working as a heat bath, was controlled to be within  $\pm 0.1$  mK. The temperature of the metal block, measured by a Pt temperature sensor, TS1, was regarded as that of the sample. If we could measure

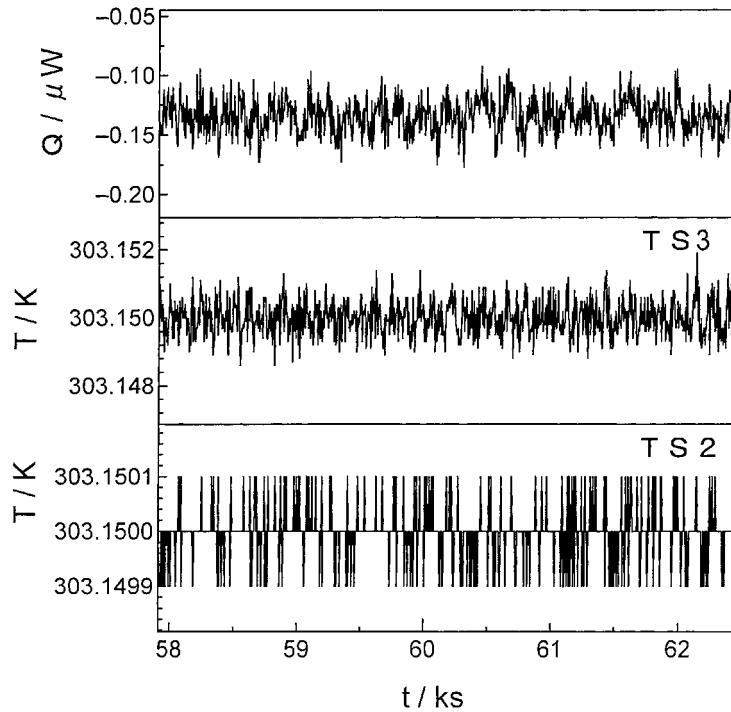


Fig. 2. Baseline fluctuation and the variation of the temperatures,  $T_{S2}$  and  $T_{S3}$  at about 303 K.

the temperature fluctuation of TS1, it would be very interesting. However, it is not possible due to the lack of enough sensitivity of TS1. There are two reasons for this. One is that the temperature fluctuation of TS1 is estimated to be extremely small, the order of  $0.01 \mu\text{K}$ , not detected by a nanovoltmeter judging from the electromotive force of the thermoelectric elements. The other reason is that the current applied to the Pt temperature sensor should be as small as possible. Otherwise, it generates heat near the sample resulting in the baseline fluctuation. Therefore, the temperature fluctuation of TS1 is not shown in Fig. 2. The baseline fluctuation of the heat flux is also shown in Fig. 2, where it is within  $\pm 25 \text{ nW}$ . The reason for such a stable baseline is due to the high sensitivity of the thermoelectric modules and due to the copper disks between TM3 and the sample, which have relatively large heat capacities and work as a dump of the temperature fluctuation resulting from the error of the temperature control of TS2 and the heat exchange with surroundings.

The temperature range of this calorimeter is limited by the thermoelectric module; from low temperature to 473 K. We have tested the measurement in the range between 100 and 453 K in a similar type of the calorimeter. Since the baseline is stable enough, the heating and cooling rate can be chosen as low as possible. However, the lowest cooling rate we have chosen is  $0.01 \text{ mK s}^{-1}$ , because it takes long time for the measurement. A high heating is not suitable in this calorimeter, since there are thick copper blocks between TM3 and sample. The highest heating rate we have chosen so far is  $10 \text{ mK s}^{-1}$  ( $0.6 \text{ K min}^{-1}$ ). The sample containers used were commercially available aluminum pans.

## 2.2. Sample

The  $\text{C}_{32}\text{H}_{66}$  sample was synthesized by using Wurtz condensation method and its purity was determined as 99.6% by gas chromatography. The sample amount used for the DSC measurement was about 2 mg.

## 3. Results and discussion

The DSC curve of heating run at a rate of  $0.4 \text{ mK s}^{-1}$  for the  $\text{C}_{32}\text{H}_{66}$  sample is shown in Fig. 3. We can see two large peaks around 339.1 and 341.9 K

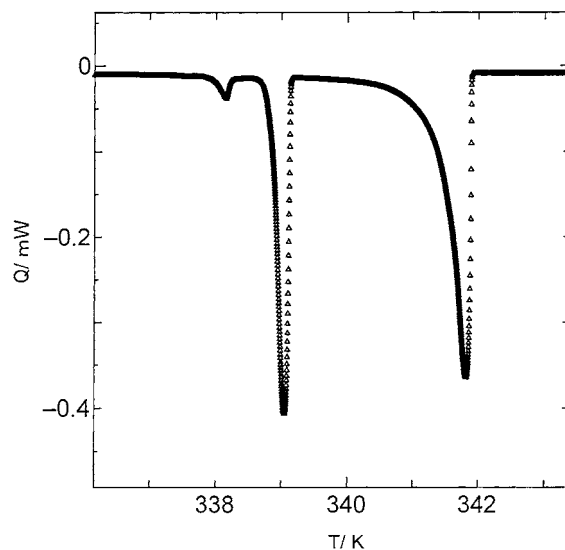


Fig. 3. DSC curve of heating run at the rate of  $0.4 \text{ mK s}^{-1}$  of  $\text{C}_{32}\text{H}_{66}$  sample.

with the enthalpy change of  $40.59$  and  $79.74 \text{ kJ mol}^{-1}$ , and the entropy change of  $119.2$  and  $232.6 \text{ J K}^{-1} \text{ mol}^{-1}$ , respectively. The former peak is known as due to the solid–solid transition from the crystalline phase in the orthorhombic form to the rotator phase, where the alkane chains undergo the unrestricted random rotation at a frequency larger than  $1000 \text{ Hz}$  holding the trans-zigzag conformation [13]. According to the X-ray scattering study by Denicolo et al. [10], in which the measurement was made in the heating direction, the rotator phase is designated as  $R_{\text{II}}$ . The molecules are aligned to be ordered but are obliquely distorted in the  $R_{\text{II}}$  phase. The latter peak is due to the transition from the rotator phase,  $R_{\text{II}}$ , to the liquid phase.

The third peak seen around  $338.1 \text{ K}$  is a newly detected one by DSC. Since Takamizawa et al. [14] found separate peaks at a few Kelvins below the melting point in the DSC curve of the even member of  $\text{C}_{36}\text{H}_{74}$ , they carefully measured the DSC curve of the  $\text{C}_{32}\text{H}_{66}$  [8,14], expecting separate peaks around  $339 \text{ K}$ , without success. Detection of the new peak in DSC shows the high resolution and high sensitivity of the present apparatus. The X-ray scattering study of  $\text{C}_{32}\text{H}_{66}$  by Sirota et al. [11] showed no significant change of the reciprocal lattice spacings in the tem-

perature range of the third peak. More recently, however, Shashikanth and Prasad [15] made a powdered X-ray diffraction study as a function of temperature on  $C_{32}H_{66}$ . They found that the lattice spacing sharply changed and the diffuse scattering rapidly increased between 333 and 341 K. They ascribed this phenomena to a highly defective stacking. Kitamaru et al. [13], Ishikawa et al. [16] and Jarrett et al. [17] studied the molecular motion of *n*-alkanes by using  $^{13}C$  NMR spectrometry and found that the molecular motion of  $CH_3$ ,  $\alpha$ - $CH_2$ ,  $\beta$ - $CH_2$  and  $\gamma$ - $CH_2$  were different from that of the internal- $CH_2$ . Some fluctuational motion around the C–C bond occurs in the vicinity of the molecular ends, even below the temperature of the rotator transition [13]. Levay et al. [18] discussed the phase transitions in  $C_{32}H_{66}$  and  $C_{33}H_{68}$  by positron annihilation techniques. They found three anomalous behaviors in the life time of positron annihilation between 330 and 340 K in  $C_{32}H_{66}$ , indicating some phase transitions. It is noted, however, they found that  $CH_3$  rotation occurred below room temperature both in  $C_{32}H_{66}$  and  $C_{33}H_{68}$ . Kim et al. [19] gave the fractional change of gauche bonds of alkanes per chain as a function of temperature from infrared spectra. The disordered gauche bonds become significant as temperature increases. Jarrett et al. [17] interpreted the premelting behavior of *n*-alkanes as due to the change of molecular motion in the vicinity of the molecular ends. Ishikawa et al. [13] observed the change of molecular motion of  $CH_3$  and  $\alpha$ - $CH_2$  between 313 and 343 K in  $C_{32}H_{66}$ . Although the mechanism of the peak found at 338.1 K is not so clear, it may be related to the disorder of the structure resulting from the active molecular motion in the vicinity of the molecular ends.

The enthalpy and entropy change of the new peak were calculated as  $2.11 \text{ kJ mol}^{-1}$  and  $6.22 \text{ J K}^{-1} \text{ mol}^{-1}$ , respectively, the both of which are 5.2% of the rotator transition. It is noted that the new peak is rather broad compared with the first and the second peaks. Such a broad peak indicates that the phase transition has a cooperative character. One of the explanation for the cooperative character of the transition would be due to an interaction among rotating  $CH_3$  ends of neighboring molecules.

The DSC curve of cooling run at the rate of  $0.4 \text{ mK s}^{-1}$  is shown in Fig. 4, where the four thermal peaks corresponding to melting, the two rotator

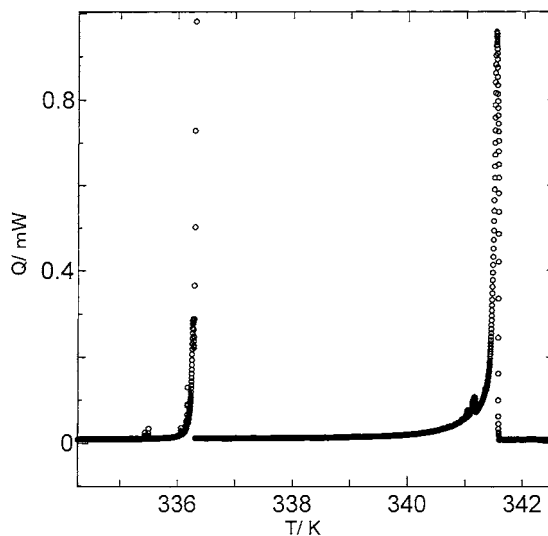


Fig. 4. DSC curve of cooling run at the rate of  $0.4 \text{ mK s}^{-1}$  of  $C_{32}H_{66}$  sample.

transitions and the new peak are seen around 341.5, 341.2, 336.2 and 335.5 K, respectively. A small peak found around 341.2 K is considered to be due to the rotator transition from  $R_{IV}$  to  $R_{III}$  [11], which was not observed in the heating process owing to the thermal hysteresis [12]. The peak seen at 336.2 K is considered to be due to the transition from  $R_{III}$  to crystal [11]. The peak seen at 335.5 K is considered to be corresponding to the new peak found at 338.2 K in the heating run. The difference in the transition temperatures of the new peak and the two rotator transitions between the heating and the cooling run is considered to be mainly due to thermal hysteresis of the sample, as observed in other *n*-alkanes [12].

The DSC curves for the solidifying process from the melting state at the cooling rate of  $0.4 \text{ mK s}^{-1}$  and  $40 \mu\text{K s}^{-1}$  are shown in Fig. 5, where several small exothermic sub-peaks are observed between 341 and 341.4 K in addition to the rotator transition from  $R_{IV}$  to  $R_{III}$  and the main solidifying peak. The sub-peaks between 341 and 341.4 K at the cooling rate of  $40 \mu\text{K s}^{-1}$  are magnified as shown in Fig. 6, where many very sharp peaks in addition to the rotator transition from  $R_{IV}$  to  $R_{III}$  at 341.2 K are seen. The detection of such small and sharp peaks indicates the quick response of the present apparatus as well as the high sensitivity and the stable baseline of the present apparatus. The

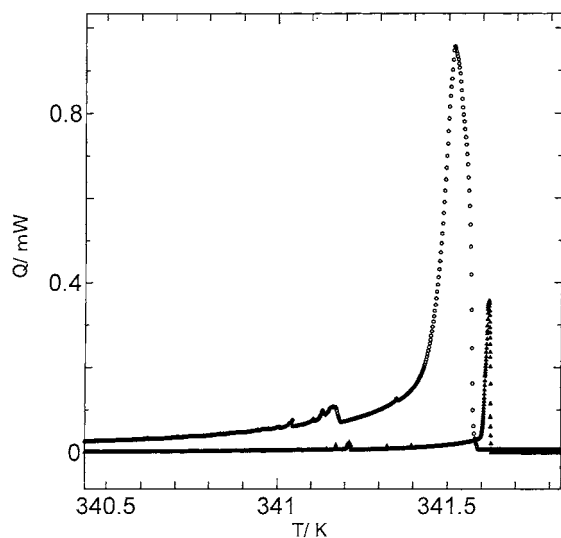


Fig. 5. DSC curve of  $C_{32}H_{66}$  sample for the solidifying process from the melting state at the cooling rate of  $0.4 \text{ mK s}^{-1}$  and  $40 \mu\text{K s}^{-1}$ .

sub-peaks, seen at about 341.3 K, for example, is magnified as shown in Fig. 7, where the temperature resolution is estimated to be about 1 mK. The heat generated in the peak shown in Fig. 7 is calculated as  $91 \mu\text{J}$ , which is very small. Around the temperature

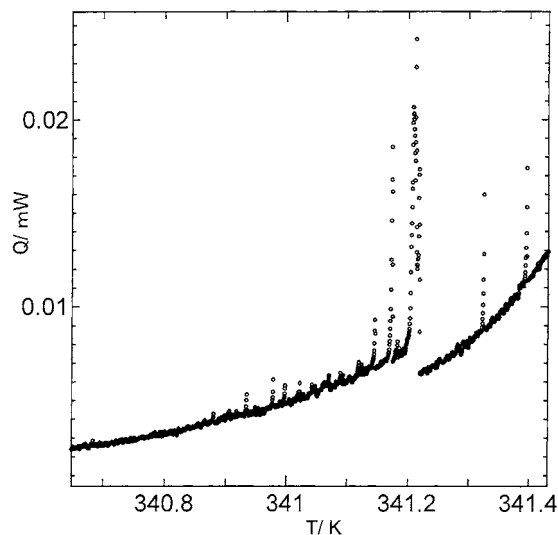


Fig. 6. The magnified DSC curve of  $C_{32}H_{66}$  sample for the solidifying process around 341 K at the cooling rate of  $40 \mu\text{K s}^{-1}$ .

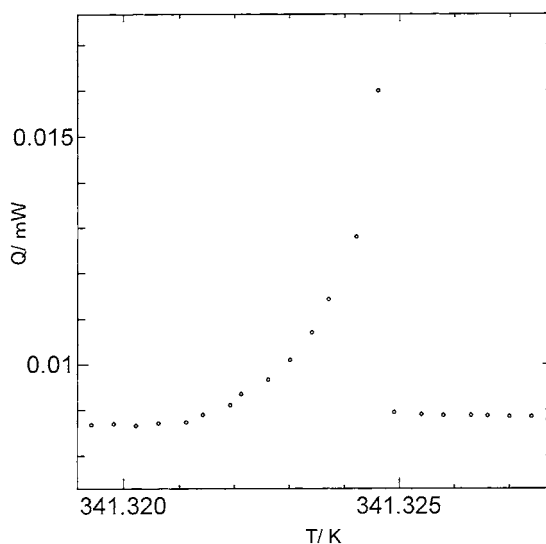


Fig. 7. The magnified DSC curve around 341.3 K in Fig. 6.

of 341.5 K in Fig. 6, the main solidifying process is already accomplished and only grain-boundary regions of each grain are considered to remain disordered, since the sample is not a single crystalline but is made of many grains with the size ranging  $10 \mu\text{m}$ . During the very slow cooling process, the solid grains intergrow by absorbing other grains, resulting in reducing the grain-boundary regions. Such an inter-growth of grains is very similar to that in the sintering process of ceramics. The grain size is distributed and the energy to make the inter-growth of grains is different depending on the grains. Therefore, the temperature and the energy released due to the inter-growth of grains is different, resulting in many exothermic sub-peaks in the DSC curve.

#### 4. Conclusions

1. A high resolution and super-sensitive DSC capable of cooling control as well as heating control has been constructed in this study. The temperature control of the calorimeter was made within  $\pm 0.1 \text{ mK}$  and the baseline fluctuation of the calorimeter was within  $\pm 25 \text{ nW}$ , and the temperature resolution of the calorimeter was estimated to be about 1 mK.

2. Phase transitions of  $n\text{-C}_{32}\text{H}_{66}$  were measured using this DSC and a small new phase transition was found as well as the known rotator transitions and the melting transition.
3. In the solidifying process from the melting state at the cooling rate of  $40\ \mu\text{K s}^{-1}$ , several small and sharp exothermic sub-peaks were observed in addition to the rotator transition and the main solidifying peak. The sub-peaks are considered to be due to ordering of the grain-boundary regions by the inter-growth of grains.

### Acknowledgements

This work has been partially supported by the Japan Society for the Promotion of Science through the Research for the Future Program.

### References

- [1] B. Wunderlich, Thermal Analysis, Academic Press, New York, 1990.
- [2] T. Hatakeyama, F.X. Quinn, Thermal Analysis: Fundamentals and Application to Polymer Science, Wiley, New York, 1994.
- [3] E.L. Charsley, S.B. Warrinton (Ed.), Thermal Analysis—Techniques and Applications, The Royal Society of Chemistry, 1992.
- [4] T. Hatakeyama, Z. Li, Handbook of Thermal Analysis, Wiley, New York, 1998.
- [5] H. Inaba, K. Tozaki, H. Hayashi, C. Quan, N. Nemoto, T. Kimura, Physica B, submitted for publication.
- [6] B. Even, G. Strobl, D. Richter, Faraday Discuss. Chem. Soc. 69 (1980) 19.
- [7] G. Strobl, B. Even, E.F. Fisher, W. Pieszek, J. Chem. Phys. 61 (1974) 5257.
- [8] Y. Urabe, K. Takamizawa, Technology Reports of Kyushu University, Vol. 67, 1994, p. 85.
- [9] Y. Urabe, M. Saito, H. Fujiwara, N. Nemoto, Technology Reports of Kyushu University, Vol. 72, 1999, p. 101.
- [10] I. Denicolo, J. Doucet, A.F. Craievich, J. Chem. Phys. 78 (1983) 1465.
- [11] E.B. Sirota, H.E. King Jr., D.M. Singer, H.H. Shao, J. Chem. Phys. 98 (1993) 5809.
- [12] E.B. Sirota, D.M. Singer, J. Chem. Phys. 101 (1994) 10873.
- [13] R. Kitamaru, F. Honi, M. Nakagawa, K. Takamizawa, Y. Urabe, Y. Ogawa, J. Mol. Str. 355 (1995) 95.
- [14] K. Takamizawa, Y. Ogawa, T. Oyama, Polym. J. 14 (1982) 441.
- [15] P.B. Shashikanth, P.B.V. Prasad, Ind. J. Eng. Mater. Sci. 7 (2000) 225.
- [16] P. Ishikawa, H. Kurosu, I. Ando, J. Mol. Str. 248 (1991) 361.
- [17] W.L. Jarrett, L.J. Mathias, R.G. Alamo, L. Mandelkem, D.L. Dorset, Macromolecules 25 (1992) 3468.
- [18] B. Levay, M. Lalovic, H. Ache, J. Chem. Phys. 90 (1989) 3282.
- [19] Y. Kim, H.L. Strauss, R.G. Snyder, J. Phys. Chem. 93 (1989) 7520.